Scientific Annals, School of Geology, Aristotle University of Thessaloniki Proceedings of the XIX CBGA Congress, Thessaloniki, Greece	Special volume 99	289-298	Thessaloniki 2010

RECORD OF TWO ALPINE HIGH-P METAMORPHIC EVENTS IN THE TITAROS OPHIOLITE COMPLEX OF THE PELAGONIAN ZONE (GREECE)

Mposkos, E.[1], Baziotis, I.[1] and Krohe, A.[2]

[1] *National Technical University of Athens, School of Mining and Metallurgical Engineering, Division of Geological Sciences, 9, Polytechniou Str., Zografou (Athens),Greece, Phone ++3021-07722099*

[2] *Institute for Mineralogy, Laboratory of Geochronology University of Muenster Corrensstr.24, D-48149 Muenster, NRW, Phone: ++49-251-8333405 email: krohe@unimuenster.de*

Abstract: We present new petrological data of the Titaros ophiolite complex and discuss their significance for the Alpine geodynamic evolution in the Pelagonian realm. There are two Alpine high-*P* metamorphic stages. The first stage, at pressures between 0.8-1.4 GPa and minimum temperatures 570-610^{0}C occurred in late Jurassic/early Cretaceous and is associated with the obduction of the ophiolite complexes onto the Pelagonian crust. At this stage the Titaros ophiolite was subducted together with crustal rocks of the Pelagonian zone as a result of tectonic erosion of the ophiolite margin. The second stage occurred in the Eocene at much lower temperatures (about 400^{0}C and minimum pressure ~0.7 GPa). It is interpreted to reflect the final closure of the Vardar-Axios ocean and collision/underthrusting of the Apulia microcontinent under Europe.

Keywords: Pelagonian zone, ophiolite complex, alpine H*P* metamorphism

1. Introduction

In Greece, the Hellenides form an integral part of the Alpine orogenic system. They have been traditionally subdivided into several NW-SE trending geotectonic zones (Fig. 1). The Pelagonian Zone, in the central part of the Hellenic orogen, consists of a) pre-Alpine crystalline basement rocks, b) Permo-Triassic volcano-sedimentary and Triassic-Jurassic platform carbonates which are only weakly metamorphosed at the western margin and more intensely metamorphosed at the eastern margin of the Pelagonian zone, c) ophiolites obducted from the Vardar-Axios zone in the late Jurassic-early Cretaceous, and d) transgressive Cretaceous limestones that upward pass into Paleocene flysch (Kilias and Mountrakis, 1989). During the early Cretaceous and Tertiary several shear zones developed referred to episodes of westward thrusting and imbrication.

The Pelagonian Zone in the Hellenic Orogene shows a Complex polymetamorphic history. The pre-Alpine basement rocks of the Vernon and Voras Massifs (Western Greek Macedonia) record a L*P*/H*T* metamorphic event associated with Carboniferous magmatic intrusions (Mposkos et al., 2001; Mposkos and Krohe, 2004). This is overprinted by two alpine metamorphic events that affected all lithologies of the Pelagonian Zone.

a: An Early Cretaceous high pressure (H*P*) metamorphism (~1.0 GPa at 500-550^{o}C), interpreted to be related to the obduction of the ophiolites onto the Pelagonian zone affected the pre-Alpine basement rocks of the eastern Pelagonian zone and the protoliths of the metapelites and metabasites of the overlying Permo-Triassic volcano-sedimentary series from Voras and Vermion massifs (Yarwood and Dixon, 1977; Schermer et al., 1990; Mposkos et al., 2001; Mposkos and Perraki, 2001; Mposkos and Krohe, 2004; Most et al., 2001). Rb-Sr isotope dating on phengites from pre-alpine gneisses in High-Pierian Mountains north of the Titaros ophiolites yielded an early Cretaceous age for this epidote-amphibolite facies metamorphism (Yarwood and Dixon, 1977).

b: An Eocene greenschist to blueschist facies metamorphism interpreted to be associated with the final closure of the Vardar-Axios ocean and collision/underthrusting of the Apulia micro-

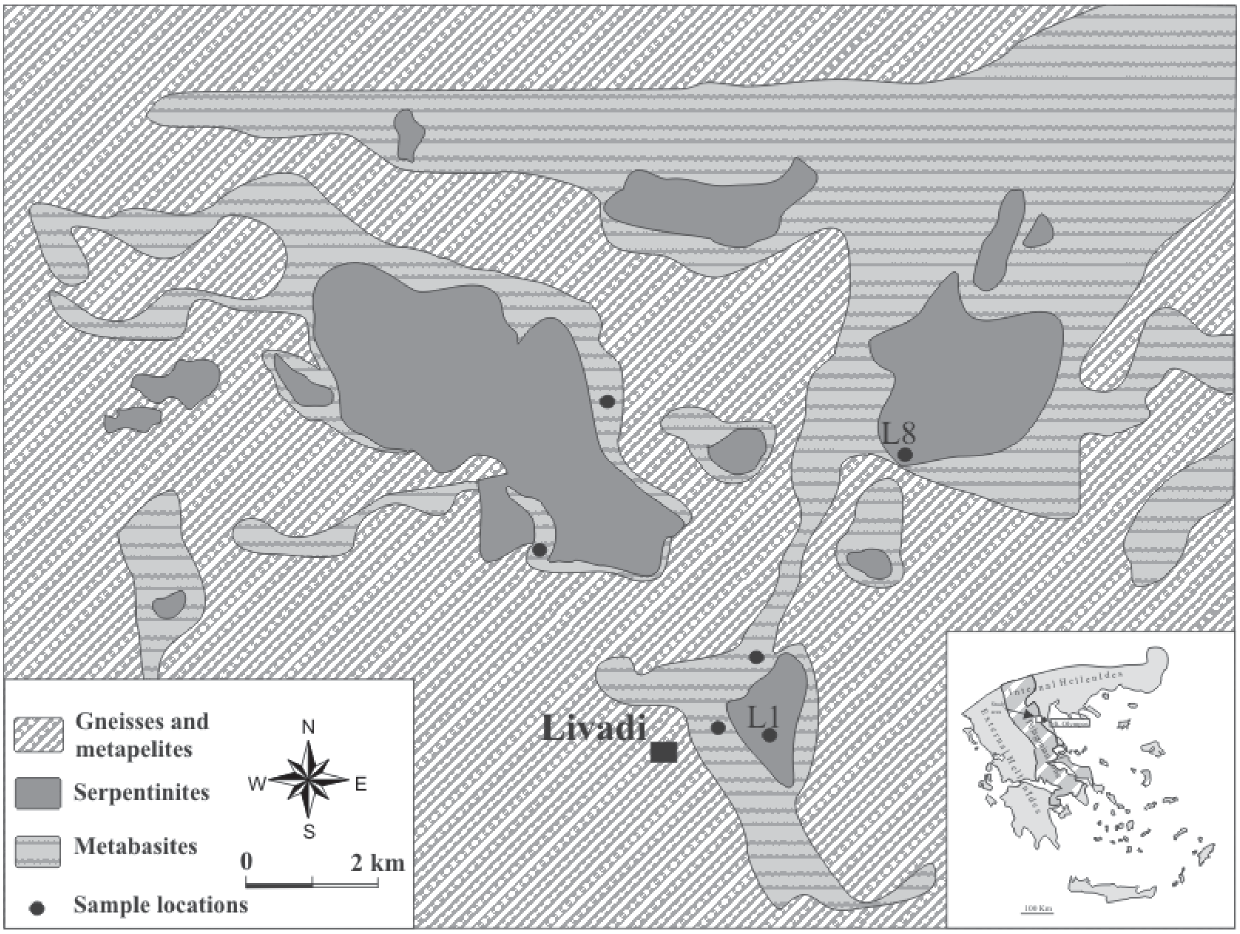

Fig. 1: Simplified geological map of the Titaros ophiolite in Livadi area (after Katsavrias 1988). Inset: Geotectonic map of Greece, showing the location of the studied area.

continent under Europe (Schermer et al., 1990), affected all rock units (including late Cretaceous sediments) of the eastern Pelagonian zone and the tectonically overlying Almopian zone (Mposkos, 1987; Mposkos and Perraki, 2001; Kilias and Mountrakis, 1985).

Enormous masses of ophiolite were sheared off from the Vardar-Axios oceanic lithosphere, obducted onto the continental Pelagonian zone and subsequently transported over large distances to the west (Laubscher and Bernoulli, 1977) over the western Pelagonian continental block. These obducted ophiolites (e.g. Pindos, Vourinos, Orthris, Central Evia ophiolites) are not pervasively affected by the early Cretaceous and Tertiary regional metamorphism, the re-equilibration being commonly limited only to metamorphic soles and the very low grade serpentinisation. An alternative model suggests that the Pindos ophiolites and those of the western Pelagonian zone derived from the Pindos Ocean obducted from west to east onto the western Pelagonian continental block in late Jurassic (e.g. Robertson, 2002 and references therein). Only the ophiolite bodies at the eastern margins of the Pelagonian zone (the Almopia ophiolites) record the Eocene greenschist to blueschist facies metamorphism, characterized by the mineral assemblages Act-Chl-Tlc-Stp-Rbk-Mt (mineral abbreviations after Martin, 1998) in late Cretaceous nickeliferous laterites formed on top of antigorite serpentinites (Mposkos, 1981) and Act-Chl-Rbk-Phg-Ab in metabasite gravels from upper Cretaceous conglomerates (Mposkos unpublished data). ^{39}Ar-^{40}Ar dating on phengites from the High Pierian date to the Eocene this metamorphism (Schermer et al., 1990).

The Titaros ophiolite both overlies pre-Alpine basement rocks and amphibolites of unknown age and within plate tholeiitic affinity (Boudi et al., 2007) or it is tectonically intercalated with them. Evidence of pre-Alpine L*P*/H*T* metamorphism like that recorded in the basement rocks is absent from the ophiolitic rocks.

In this work we present mineral assemblages and mineral compositions from the Titaros ultramafic body, the former serpentinized base of the obducted ophiolite, and the underlying albite-epidote amphibolites from the Livadi area (west to the Olympus Mountain), which represent together with the pre-Alpine continental crust the subducted plate. We will show that the Titaros Ophiolite records two metamorphic events. (1) Early Cretaceous H*P* metamorphism associated with the obduction of the ophiolite onto the Pelagonian continental margin. At that time the Titaros Ophiolite was incorporated into the underlying basal unit by tectonic erosion thus both experienced a common prograde H*P* metamorphism. (2) Tertiary H*P*/L*T* metamorphism associated with the final closure of the Vardar/Axios ocean.

2. Geological Setting

In the Livadi area (Fig. 1) the Pelagonian zone is predominantly composed of pre-Alpine two mica gneisses, migmatitic gneisses, granitoid gneisses and epidote-mica schists representing the pre-Alpine basement. These are overlain by up to 300m thick light to dark green albite-epidote amphibolites forming the basal unit of the Titaros ophiolite. Local thin interlayers of garnet-bearing two mica schists represent former oceanic sediments. Both lithological associations exhibit a consistent and a well developed foliation and lineation. Serpentinized peridotites, showing local concentrations of chromite ore, overlie the albite-epidote amphibolites. Dark colored metadiabase dykes, ~ 20 to 30 cm thick, intrude the peridotite.

Owing to the Tertiary tectonics the Titaros ophiolite is imbricated within the pre-Alpine mylonitic gneisses. Mineral stretching lineation and kinematic indicators of the basement gneisses and the albite-epidote amphibolites are consistent with a WSW transport in accordance with the Tertiary tectonic nappe transport direction in the Hellenic orogen.

3. Petrography

3.1. Metaperidotite: The less serpentinized metaperidotites show harzburgitic (olivine, talc, antigorite, tremolite, chlorite, chromite, Ni-sulfides e.g. metaharzburgite samples; L1 in figure 1) or dunitic (olivine, antigorite, chromite and magnetite e.g. metadunite samples; L8 in figure 1) compositions.

Two generations of olivine occur: (i) larger crystals (~ 4 mm in size, Ol-1) with undulatory extinction and deformation bands. (ii) finer grained aggregates of newly formed olivine crystals (0.05-0.1 mm in size, Ol-2), developed along the grain boundaries and the deformation planes crosscutting the Ol-1.

Ol-1 contains inclusions of antigorite, talc, tremolite and chlorite (Fig. 2a) and is in microstructural equilibrium with matrix talc and tremolite. Pockets of finer grained olivine, which consist of granoblastic polygonal aggregates in microstructural equilibrium with talc and tremolite are considered as aggregates of Ol-2 formed at low differential stress (Fig. 2b).

Three generations of talc are distinguished based on microstructural criteria: a) talc inclusions in Ol-1 (Fig. 2c). A shape preferred orientation of talc inclusions depicts a foliation older than the growth of the olivine. b) Large flakes of talc in the matrix in microstructural equilibrium with olivine. Bending and kinking of talc flakes indicate deformation after olivine and talc growth. c) Pockets of retrograde fine grained talc aggregates intergrown with chlorite, antigorite and ferrit-chromite replacing olivine (Fig. 2d).

Antigorite inclusions (Atg-1) in Ol-1 are associated with talc and chlorite. Antigorite inclusions mostly do not show preferred orientation except for some laths that are oriented parallel to the (010) and (001) crystal faces of the host olivine. Matrix antigorite (Atg-2) either grew as random oriented flakes replacing Ol-1 or as pockets associated with retrograde fine-grained talc, prismatic tremolite and ferrit-chromite grains. Commonly retrograde antigorite and talc replace Ol-1 along dislocation of deformation bands.

Chromite grains are zoned (see mineral chemistry) showing a dark grey core and lighter rim in SEM images. At their rims they are replaced by intergrowths of chlorite and ferrit-chromite.

3.2. Dyke amphibolites: Up to 30 cm thick dark green dykes are preserved, which originally intrude the peridotite. They are now composed of brownish-green amphibole (> 80 vol%) (0.1 to 0.3 mm in size), albite, omphacite, titanite and ilmenite. The amphiboles are zoned with a blue-green rim. Omphacite is observed only as inclusions in brownish-green amphibole cores (Fig. 2e). A shape preferred orientation of prismatic amphibole define a lineation.

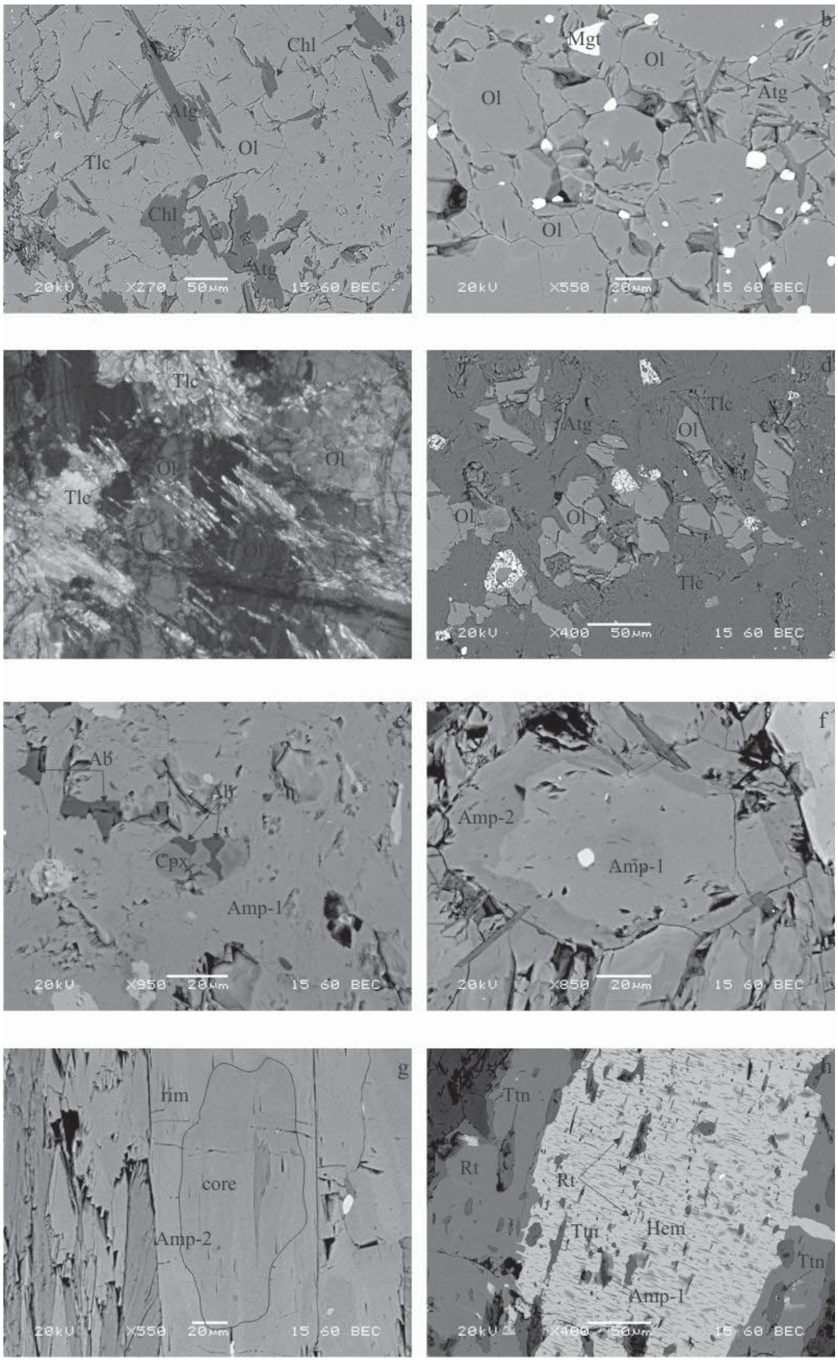

Fig. 2: (a) Inclusions of antigorite (Atg), talc (Tlc) and chlorite (Chl) in larger olivine crystals (Ol-1). SEM Back Scattered Electron (BSE) image. (b) Aggregate of olivine grains with granoblastic polygonal microstructure. SEM BSE image. (c) Inclusions of oriented talc flakes oriented in large olivine crystal (Ol-1). Photo-micrograph, crossed polars. Large olivine crystal (Ol-1) showing deformation twins. (d) Aggregate of talc (Tlc) and antigorite (Atg) flakes replacing olivine (Ol). Olivine grains show corroded edges. White grains are ferrit-chromite in intergrowth with antigorite. SEM BSE image. (e) Omphacite (Cpx) associated with albite (Ab) included in hornblende (Amp-1)(dyke amphibolite in metaperidotite). SEM BSE image. (f) Amp-1 is overgrown by Amp-2. SEM BSE image. (g) Amp-2 with compositional zoning. SEM BSE image. (h) Ilmeno-hematite with lanse shaped rutile (Rt) exsolutions/segregations. Inclusions of amphibole (Amp-1) are rimmed by titanite (Ttn).

3.3. Albite-epidote amphibolite and epidote hornblendite: The mineral assemblage of the albite-epidote amphibolite of the basal unit is Hbl+Czo+Chl+Phg+Ab+Ttn+Rt+Qtz and that of the epidote hornblendite is: Amp+Ep/Czo+Chl+Phg+Rt+Ttn+Ilm-Hem. Both rocks show a well developed lineation defined by the long axis preferred orientation of amphiboles and epidote grain elongation.

Two amphibole generations are distinguished based on microstructural criteria in thin sections and compositional zoning of individual grains (see mineral chemistry). The first generation (Amp-1) has a green to brownish-green color and occurs as inclusions in hematite, allanite and rutile. The second generation (Amp-2: Fig. 2g) either occurs in the rock matrix or as overgrowths of Amp-1 overgrowths (Fig. 2f). Amp-2 shows zoning with a colorless core and a blue-green rim. Epidote is zoned with colorless to yellow-greenish core and green rim. In albite-epidote amphibolite the main accessory phase is titanite, which is formed at the expense of former rutile still preserved as inclusion. In the epidote hornblendite, titanite is included in hematite and rutile (Ttn-1). In the rock matrix titanite is formed at the expense of rutile (Ttn-2). Ilmeno-hematite (see mineral chemistry) contains lance-shaped rutile exsolutions/segregations (Fig. 2h) and rutile that is formed replacing hematite contains needle-like segregations of hematite.

4. Mineral chemistry

Representative samples of metaperidotites, dyke amphibolites and amphibolites from the basal unit were selected to determine the mineral chemistry. Analyses were performed using a JEOL 6380 LV SEM equipped with energy dispersive system (EDS) at the School of Mining and Metallurgical Engineering, National Technical University of Athens. In ilmeno-hematite grains spot analyses were performed in areas free of rutile exsolutions. The beam-scanning technique was also used for analyzing bulk chemical composition of hematite-rutile intergrowths in domains of former Ti-richer ilmeno-hematite that now consist of Ti-poorer ilmeno-hematite + lance-shaped rutile inclusions. Representative mineral compositions are given in table 1.

***4.1. Metaperidotite*:** *Olivine* ($Fo_{0.90-0.93}$) is homogeneous in composition regardless of grain size. The NiO content in olivine ranges from 0.12 to 0.14 wt%. *Tremolite* is low in aluminum. The Al_2O_3 content ranges from below the detection limit up to 0.73 wt%. Tremolite grains which are in microstructural equilibrium with olivine show higher Al_2O_3 contents. The Mg/(Mg+Fe) ratio in tremolite ranges from 0.90 to 0.97. *Talc* has the highest Mg/(Mg+Fe) ratio (0.98-0.99) of all the silicate minerals in the metaperidotite. The Al_2O_3 and Cr_2O_3 content in *antigorite* ranges from below the detection limit up to 2.26 wt% and 2.68 wt%, respectively. The FeO content ranges from 2.37 to 3.69 wt%. *Chlorite* is clinochlore with 6.508 to

Table 1. Representative compositions of amphibole (Amp), omphacite (Cpx), ilmeno-hematite (Ilm-Hem), spinel (Spl), ferrit-chromite (Fe-Chr), Cr-magnetite (Cr-Mgt) and phengite (Phg).

	Amp-1 core	**Amp-1 rim**	**Amp-2 core**	**Amp-2 rim**	**Cpx**	**Ilm-Hem**	**Ilm-Hem**	**Spl-1**	**Fe-Chr**	**Cr-Mgt**	**Phg**
SiO_2	51.56	44.46	54.63	52.97	55.86	-	-	-	-	-	51.04
TiO_2	0.43	0.53	-	0.15	-	18.35	10.96	-	-	-	-
Al_2O_3	4.85	10.66	1.37	4.03	11.72	-	-	15.04	-	-	23.67
Cr_2O_3	-	-	-	-	-	0.20	-	52.92	48.92	18.00	-
Fe_2O_3	1.08	-	0.11	2.48	0.24	65.15	79.19	1.29	20.30	51.43	-
FeOt	12.86	16.45	11.61	11.28	5.74	16.50	9.85	24.12	28.91	29.15	5.08
MnO	-	-	-	0.93	-	-	-	-	-	-	-
MgO	13.47	9.94	16.29	13.37	6.72	-	-	6.77	1.88	1.40	3.75
CaO	11.28	10.91	12.69	9.98	12.15	-	-	-	-	-	-
Na_2O	1.31	3.45	0.39	2.09	7.26	-	-	-	-	-	-
K_2O	0.16	0.62	-	-	-	-	-	-	-	-	11.47
Total	97.02	97.02	97.10	97.13	99.70	100.00	100.00	100.15	100.01	99.98	95.09
(O)	23	23	23	23	6	3	3	4	4	4	22
Si	7.512	6.702	7.864	7.675	2.000	-	-	-	-	-	6.971
Ti	0.048	0.060	-	0.016	-	0.360	0.217	-	-	-	-
Al	0.832	1.894	0.233	0.688	0.495	-	-	0.586	-	-	3.809
Cr	-	-	-	-	-	0.004	-	1.382	1.434	0.538	-
Fe^{+3}	0.118	-	0.012	0.270	0.006	1.276	1.566	0.032	0.566	1.462	-
Fe^{2+}	1.567	2.074	1.398	1.367	0.172	0.360	0.217	0.667	0.986	0.921	0.580
Mn	-	-	-	-	-	-	-	-	-	-	-
Mg	2.926	2.234	3.495	2.887	0.359	-	-	0.333	0.100	0.079	0.763
Ca	1.760	1.762	1.958	1.549	0.466	-	-	-	-	-	-
Na	0.371	1.007	0.108	0.586	0.504	-	-	-	-	-	-
K	0.031	0.120	-	-	-	-	-	-	-	-	2.000

6.924 Si atoms per formula unit (a.p.f.u.), 2.081-2.931 Al a.p.f.u. and Mg/(Mg+Fe) ratio ranging from 0.93 to 0.96.

The *spinel group minerals* show a great variety in their chemical compositions (Fig. 3). *Primary* (mantle) *chromites* are Al-chromites with $Cr/(Cr+Al+Fe^{3+})$ ratio in the range of 0.62 to 0.74 and $Mg/(Mg+Fe^{2+})$ ratio in the range of 0.23 to 0.40 and are represented by the core composition in zoned grains. Toward the rim, the composition of chromite changes to iron rich members forming *ferrit- chromites* and rarely Cr-magnetites indicating change in composition under oxidized conditions. The MgO and Al_2O_3 contents in the chromite core range from 5.63 to 7.77 wt% and 12.48 to 17 wt%, respectively; in ferrit-chromite rim they are reduced to 3.05-1.06 wt% and 2.55-0.2 wt%, respectively. Cr-magnetite occurs as inclusions in olivine grains and forms the outermost rim composition in chromite grains of the metadunite sample L8. Cr-magnetite is common in serpentinized peridotites at greenschist facies, and ferrit-chromite at amphibolite facies conditions, within the olivine+talc stability field (Evans and Frost, 1975). The Cr-magnetite inclusions in olivine indicate that they were formed at an early stage of the prograde path of metamorphism (Mgt-1), while the Cr-magnetite compositions at the rim of zoned chromite grains were formed at a retrograde stage of metamorphism (Mgt-2).

***4.2. Dyke Amphibolites*:** In these rocks, the presence of omphacite indicates that the metaperidotite underwent high pressure metamorphism. Omphacite is present only as inclusions in calcium rich amphibole (Fig. 2e). The jadeite component in omphacite ranges from 30 to 50%, and the aegirine component from 0 to 5%. In zoned omphacite grains, the jadeite component decreases from the core to the rim. The green-brown amphiboles are pargasitic hornblendes with a glaucophane component ranging from 7.1 to 30.7 %. Very rarely, the green-brown amphiboles show compositional zoning with increasing Al_2O_3 and Na_2O contents increasing from 3.44-7.92 wt% and 1.35-2.54 wt% in the core to 10.66-11.81 wt% and 3.45-3.61 wt% at the rim, respectively, indicating amphibole growth with increasing metamorphic grade. The increase in the edenite component from the core to the rim in zoned green-brown amphibole grains and the high edenite component in the homogeneous grains (Fig. 4c) is more sensitive to temperatures than pressures (Laird and Albee 1981). Obviously, the pargasitic hornblende, which is in microstructural equilibrium with albite, was formed at the expense of omphacite during decompression. At the outermost rim, the green-brown pargasitic hornblende is replaced by a blue-green amphibole showing an increase in the glaucophane and decrease in the edenite component (Fig. 4B,C), formed at the expense of matrix albite. In samples where most of the green-brown amphibole grains show blue-green rims, albite is almost absent, while albite is common in samples, in which the blue-green rims in the green-brown amphiboles are relatively rare. An increase in glaucophane component in calcic amphibole indicates pressure increase (Laird and Albee, 1981). The blue-green

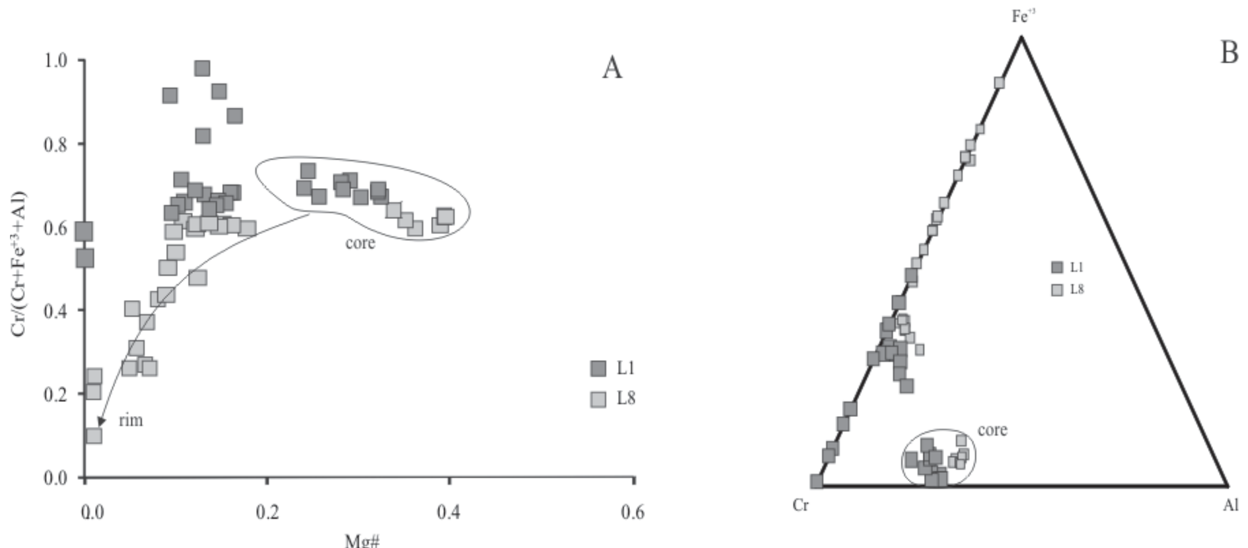

Fig. 3: (a) $Cr/(Cr+Fe^{+3}+Al)$ vs. $Mg/(Mg+Fe^{+2})$ and (b) Plots of metaperidotite spinels (Samples L1 and L8) in the Cr-Fe^{+3}-Al diagram.

amphibole rims probably record the second (Eocene) H*P*/L*T* metamorphic event (Mposkos, 1987). Albite is the pure end-member, ilmenite is Mn-bearing with pyrophanite component ranging from 9 to 11%. The Al_2O_3 content in titanite ranges from 0.47 to 0.58 wt%.

4.3. Albite-epidote amphibolite and epidote hornblendite: The two amphibole generations distinguished by microstructural criteria also show differences in the chemical composition (Fig. 4). Amp-1 is a magnesiohornblende, with glaucophane component ranging from 3 to 15%. Characteristic is a compositional zoning with an increase in Al_2O_3 content from 5.72 to 6.51 wt% in the core to the 9.01-9.12 wt% at the rim. Amp-2 is a Na-bearing tremolite with sodic amphibole component in the core ranging from 0.3 to 11% and tremoliltic hornblende with sodic amphibole component up to 25% at the rim (Fig. 4e) indicating a growth during a pressure increase (Laird and Albee, 1981). The respective compositions, chemical zoning, and microstructural relationships of the two calcic amphibole generations are compatible with amphibole growth during two prograde metamorphic episodes.

The Si content in phengite ranges from 6.73 to 6.97 a.p.f.u. and ($Mg+Fe^{2+}_{tot}$) from 1.086 to 1.36 a.p.f.u. The excess ($Mg+Fe^{2+}_{tot}$) beyond the requirement of the celadonitic substitution (0.73-0.97) indicates that most of the iron must be triva-

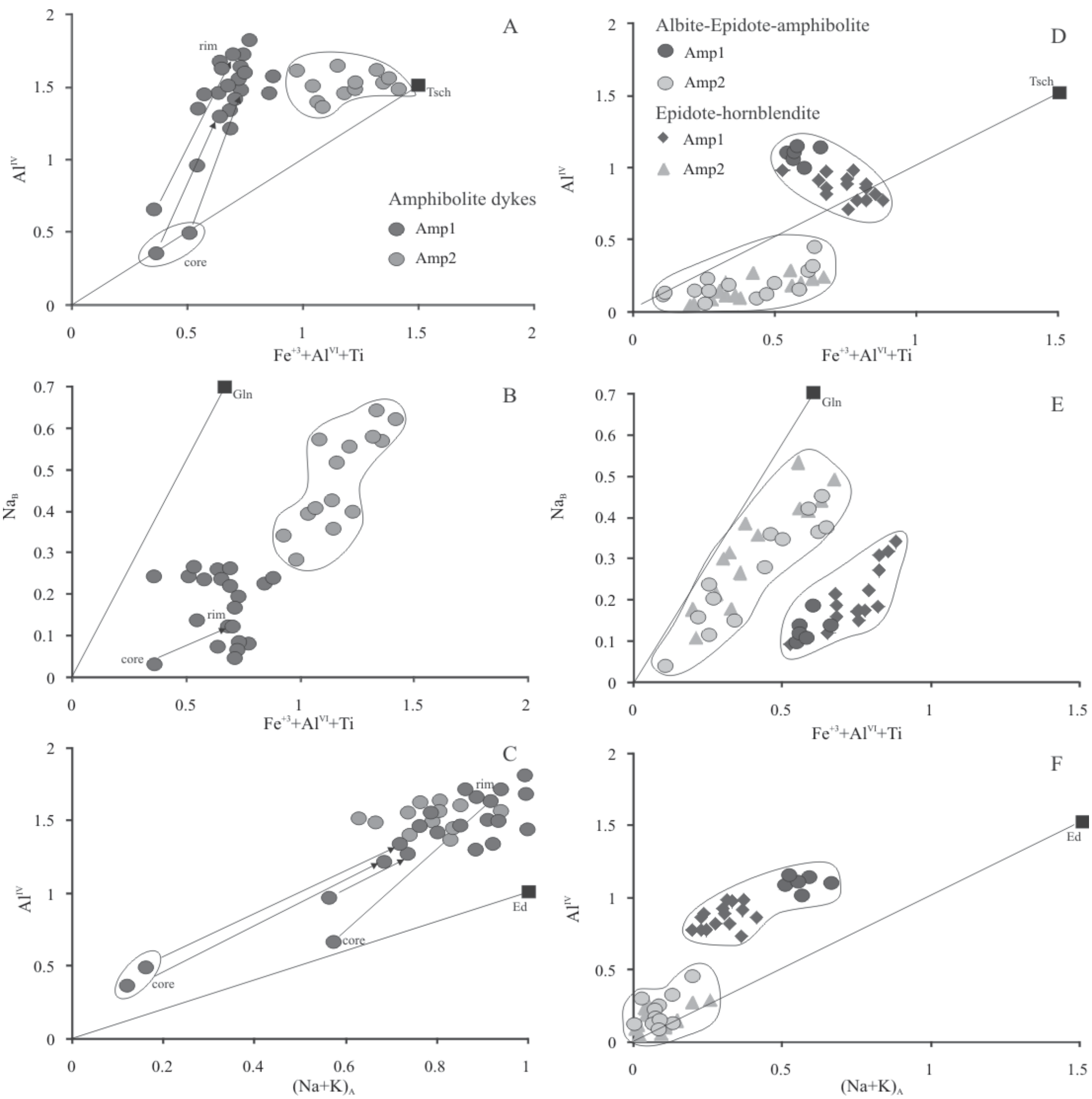

Fig. 4. Compositional variation in amphiboles from dyke amphibolites within the metaperidotite and from albite-epidote amphibolite and epidote hornblendite underlying the metaperidotite. (a) Al^{IV} vs $Fe^{+3}+Al^{VI}+Ti$, (b) Na_B vs. $Fe^{+3}+Al^{VI}+Ti$ and (c) Al^{IV} vs. $(Na+K)_A$ diagrams. Lines show the tschermakite, glaucophane and edenite component respectively, for reference.

lent, substituting for Al. Albite is pure albite and chlorite is clinochlore with Mg/(Mg+Fe) ratio ranging from 0.59 to 0.65. Epidote shows compositional zoning with increasing pistacite component from 26% in the core to 32% at the rim. In titanite the Al_2O_3 content ranges from 0.62 to 1.95 wt% and the FeO_{tot} from 0.56 to 1.43 wt%. In rutile the FeO_{tot} content ranges from 0.63-1.01 wt%. The chemistry of the ilmeno-hematite is complex because of the very fine lance-shaped rutile exsolutions/segregations. The ilmenite content of the primary ilmeno-hematite (Hem-1)(including the rutile exsolutions/segregations) varies from 32 to 37%. and that of the ilmeno-hematite domains, which are free of rutile exsolutions/segregations (Hem-2) from 21 to 26% This decrease in ilmenite component in Hem-1 and the formation of the rutile occurred in a retrograde stage of metamorphism under oxidizing conditions.

5. Metamorphic conditions

Microstructural relationships, mineral assemblages and mineral compositions in the metaperidotite and the associated metabasites (dyke amphibolites and basal amphibolites) indicate that the Titaros ophiolite is affected by two distinct prograde metamorphic events. The first at albite-epidote amphibolite facies and the second at greenschist facies conditions. The prograde character of the first metamorphic event is preserved in the metaperidotite and the chemical composition/zonation of Amp-1 in the dyke amphibolites and that of the second one in the chemical composition/zonation of Amp-2 in the albite-epidote amphibolites and epidote hornblendites of the basal unit.

The inclusions of antigorite, talc, and chlorite in Ol-1 from the metaperidotite (Fig. 2a,b) and the omphacite inclusions in amphiboles from the dyke amphibolites within the metaperidotite (Fig. 2e) demonstrate very convincingly the prograde character of the first metamorphic event that occurred at high pressures. Before that, the metaperidotite was a serpentinite with the mineral assemblage Atg+Tlc+Chl(+Di) in the metaharzburgite (sample L1) and Atg+Cr-Mgt+(Brc?) in the metadunite (sample L8) formed at low metamorphic grade. Only chromite is a relict phase from the mantle protolith. With increasing metamorphic grade olivine is formed in the metadunite at the expense of antigorite and brucite.

In metaharzburgite tremolite is formed according to the reaction:

$$\text{Atg+8Di} \rightarrow \text{18Ol+4Tr+27H}_2\text{O} \qquad (1)$$

and antigorite is decomposed to olivine+talc according to the reaction:

$$\text{Atg} \rightarrow \text{18Ol+4Tlc+27H}_2\text{O} \qquad (2)$$

P-T conditions did not exceed the stability field of olivine+talc as suggested by the stable coexistence of matrix olivine and talc. Orthopyroxene is not present in the metaperidotite. The coexistence of olivine+talc and the absence of orthopyroxene constrain the peak metamorphic conditions in the field confined by the reaction curves 2 and 5 (Fig. 5). The intersection of the above reaction curves with that of reaction 7 (Fig. 5) constrains the upper pressure limit to 1.4 GPa.

In the dyke amphibolites within the metaperidotite omphacite is present as inclusions in pargasitic hornblende and shows corroded edges (Fig. 2e). It is found in association with albite, but never with quartz. Moreover quartz is not present in the dyke amphibolites either as inclusion in amphibole or in the matrix. Therefore, quartz did probably not coexist with omphacite at the peak pressure conditions. During decompression the jadeite component in omphacite was decomposed to albite and nepheline that reacted with the amphibole to increase the edenite component in the amphibole. Hence, the peak metamorphic conditions can be constrained within the *P-T* field given from the reaction curves 2, 5, 6 and 7 in figure 5.

Minimum temperature of 570^0C is suggested by the composition of the primary ilmeno-hematite in the epidote hornblendite from the basal unit (Table 1 analysis 6), using the hematite-ilmenite solvus from Braun and Raith (1985), as ilmeno-hematite does not coexist with hemo-ilmenite.

The second metamorphic imprint is well documented by the new formation of Na-bearing actinolite and actinolitic hornblende overgrowing pargasitic hornblende from the first metamorphic event in albite-epidote amphibolites and epidote hornblendites (Fig. 2f). The increase in the glaucophane component from the core to the rim of zoned grains (Figs. 4) indicates prograde path of metamorphism at increasing pressure (Laird and Albee, 1981). Temperatures of ~400^0C are constrained using the composition of the ilmeno-hematite intergrown with rutile, assuming that ilmeno-hematite (Table 1, analysis 7) with the rutile segregations is reequilibrated at the second metamorphic event. For the above temperature minimum pressures of 0.7 GPa can be estimated from the Si-content

(Si=6.97 a.p.f.u.) of the associated phengites (Massonne and Szpurka, 1997). Probably during this metamorphic event formed the fine-grained talc, antigorite and ferrit-chromite aggregates replacing olivine in the overlying metaperidotite (Fig. 2d) formed favored by the influxof water under oxidized conditions.

6. Discussion and Conclusions

The Titaros ophiolite shows a post-emplacement history that is completely different to that recorded in all known ophiolite bodies of the Pelagonian zone (including the Almopia ophiolites at the eastern slopes of the Pelagonian zone).

Based on petrological data, two prograde metamorphic events have been recognized in the Titaros ophiolite, that are absent from the ophiolites of the western Pelagonian zone. These metamorphic events are similar in metamorphic type and grade to the early Cretaceous and Eocene metamorphic event respectively recorded in the pre-Alpine and Permo-Triassic continental protoliths of the eastern Pelagonian zone.

In the first metamorphic event peak pressures between 0.8 and 1.4 GPa and minimum temperatures of 570-610 ^{0}C are constrained from the intersection of the reaction curve 2 with those of the reactions 6 and 7 (Fig. 5). Minimum temperatures of 570 are obtained from the composition of primary ilmeno-hematite in the epidote hornblendite from the basal unit. *P-T* conditions of 500-550 ^{0}C and ~0.9-1.0 GPa are constrained for the early Cretaceous metamorphic event in the phengite orthogneisses and the overlying garnet-chloritoid-phengite schists from the south Vermion Mountain lying to the north of the Titaros Mountain (Mposkos and Perraki, 2001).

We consider that the first metamorphic event in the

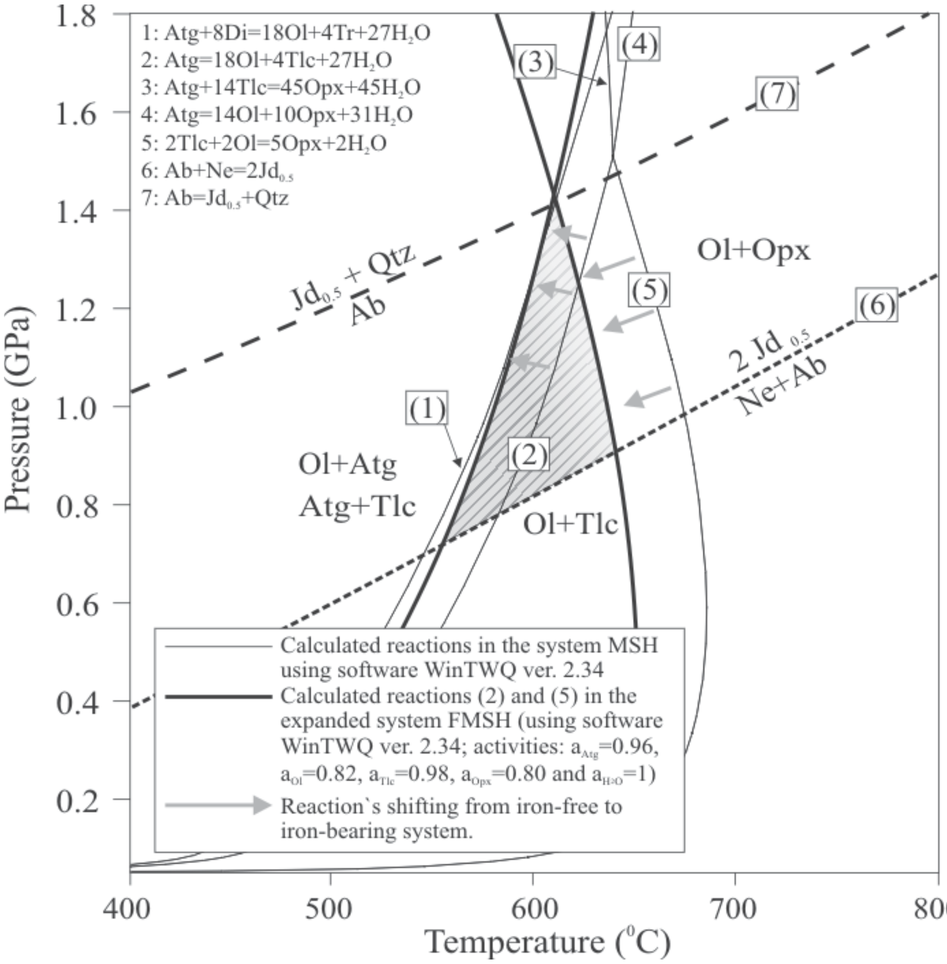

Fig. 5. *P-T* diagram showing reaction curves in the systems CaO-MgO-SiO_2-H_2O and FeO-MgO-SiO_2-H_2O calculated using real mineral compositions for olivine, talc and antigorite to constrain the peak metamorphic condition of the first metamorphic event in the Titaros metaperidotite. Reaction curves Ab+Ne→$Jd_{0.5}$ and Ab →$Jd_{0.5}$+Qtz are calculated for omphacite ($Jd_{0.5}$), pure albite and nepheline.

Titaros ophiolite may have been coeval with the early Cretaceous metamorphism recorded in the underlying crustal rocks, which occurred during the obduction of the Vardar-Axios ophiolites over the Pelagonian continental block. The Titaros ophiolite represents a slice of the obducted oceanic lithosphere (containing serpentinized peridotites) which through a tectonic erosion mechanism was detached from the overriding plate and incorporated into the subducted lower plate.

The second metamorphic event at H*P*/L*T* greenschist facies conditions (~0.7 GPa/ 400^0C) is connected with the final closure of the Vardar-Axios Ocean and the amalgamation of the Pelagonian zone to the European plate in early Tertiary (Schermer et al. 1990).

Acknowledgments

The reviewers R. Compagnoni, F. Pomoni and an anonymous one, are gratefully acknowledged for their helpful suggestions. We want to express our sincere thanks to R. Compagnoni for his linguistic handling helping to improve the manuscript.

References

Boudi, D., Prophitis E., Zachariadis P., Kostopoulos D., Baltatzis E. and Chatzitheodoridis E. 2007. Petrology, geochemistry and geotectonic setting of the Titaros ophiolite and associated Pelagonian basement rocks in the area NW of Mt. Olympos, Greece. Bulletin of the Geological Society of Greece, 40, 676-689.

Braun E. and Raith M. 1985. Fe-Ti oxides in metamorphic basites from the eastern Alps, Austria: a contribution to the formation of solid solutions of natural Fe-Ti oxide assemblages. Contributions to Mineralogy and Petrology, 90, 199–213.

Katsavrias N. 1988. Geological map of Greece. Scale 1:50000. Sheet Livadhion.

Kilias A. and Mountrakis D. 1985. Das Rizomata-Fenster im nordoestlichen Pieria-Gebirge Neue Daten zur geologischen Grenze der Pelagonischen und der Axios-Zone in Griechenland. Neues Jahrbuch fuer Geologie und Palaeontologie Monatshefte, 249-256.

Kilias A. and Mountrakis D. 1989. The Pelagonian nappe. Tectonics, metamorphism and magmatism. Bulleting of the Geological Society of Greece, 23/1, 29-46.

Laird J. and Albee A. 1981. Pressure, temperature and time indicators in mafic schists. Their application to reconstructing the polymetamorphic history of Vermont. American Journal of Science, 281, 127-175.

Laubscher H.P. and Bernoulli D. 1977. Mediterranean and Tethys. In: Nairn, A.E.M., Kanes, W.H. and Stehli, F.G. (Eds.), The Ocean basins and margins, 4/A, *The Eastern Mediterranean*, Plenum, New York, 1-28.

Martin R.F., 1998. Symbols of the rock-forming minerals. The Nomenclature of minerals: A compilation of IMA reports. IMA`98 Toronto, 148-149.

Massonne H.-J. and Szpurka Z.. 1997. Thermodynamic properties of white micas on the basis of high-pressure experiments in the systems K_2O-MgO-Al_2O_3-SiO_2-H_2O and K_2O-FeO-Al_2O_3-SiO_2-H_2O. Lithos, 41, 229-250

Most T., Frisch W., Dunkl I., Kadosa B., Boev B., Avgerinas A. and Kilias, A. 2001. Geochronological and structural investigations of the northern Pelagonian crystalline zone. Constraints from K-Ar and zircon and apatite fission track dating. Bulletin of the Geological Society of Greece, 34/1, 91-95.

Mposkos E. 1981. The Ni-Fe laterite ores of Almopia zone. UNESCO. An International Symposium on metallogeny of mafic and ultramafic complexes. Athens 1980, 1, 317-337.

Mposkos E. 1987. The chemical composition of calcic and sodic-calcic amphiboles in metabasic rocks from the Pelagonian Zone (Greece) as indicator of pressure and temperature. Chemie der Erder, 46, 161-169.

Mposkos E., Kostopoulos D. and Krohe A. 2001. Low P/T pre-Alpine metamorphism and medium-P alpine overprinting of Pelagonian Zone documented on high alumina metapelites of the Vernon Massif, Western Macedonia, Northern Greece. Bulleting of the Geological Society of Greece, 34, 949-958.

Mposkos E. and Perraki M. 2001. High pressure Alpine metamorphism of the Pelagonian allochthon in the Kastania area (Southern Vermion), Greece. Bulletin of the Geological Society of Greece, 34, 939-947.

Mposkos E. and Krohe A. 2004. New evidences of low-P/high-T pre-Alpine metamorphism and medium-P Alpine overprint of the Pelagonian zone documented in metapelites and Orthogneisses from the Voras Massif, Macedonia, Northern Greece. Bulletin of the Geological Society of Greece, 36, 558-567.

Robertson A. 2002. Overview of the genesis and emplacement of Mesozoic ophiolites in the eastern Mediterranean Tethyan region. Lithos, 65, 1-67.

Schermer E.R., Lux D.R. and Burchfield B.C. 1990. Temperature-time history of subducted continental crust, Mount Olympos region, Greece. Tectonics, 9, 1165-1195.

Yarwood G.A. and Dixon J.E. 1977. Lower Cretaceous and younger thrusting in the Pelagonian rocks of High Pieria, Greece. Colloquium of the Aegean Region, Athens 6th, 1, 269-280.